AWARD NUMBER: W81XWH-14-1-0006

TITLE: Preventing Ototoxic Synergy of Prior Noise Trauma during Aminoglycoside Therapy

PRINCIPAL INVESTIGATOR: Hongzhe Li, PhD

RECIPIENT: Loma Linda Veterans Association for Research and Education
Redlands, CA

REPORT DATE: December 2020

TYPE OF REPORT: Annual Report

PREPARED FOR: U.S. Army Medical Research and Materiel Command
Fort Detrick, Maryland 21702-5012

REPORT DOCUMENTATION PAGE

Form Approved
OMB No. 0704-0188

1. REPORT DATE *(DD-MM-YYYY)*	**2. REPORT TYPE**	**3. DATES COVERED** *(From - To)*
December 2020	Annual Report	01Dec2019-30Nov2020

4. TITLE AND SUBTITLE

Preventing Ototoxic Synergy of Prior Noise Trauma during Aminoglycoside Therapy

5a. CONTRACT NUMBER
W81XWH-14-1-0006

5b. GRANT NUMBER
11243004

5c. PROGRAM ELEMENT NUMBER

6. AUTHOR(S)

Hongzhe Li, PhD

E-Mail: Hongzhe.Li@va.gov

5d. PROJECT NUMBER

5e. TASK NUMBER

5f. WORK UNIT NUMBER

7. PERFORMING ORGANIZATION NAME(S) AND ADDRESS(ES)

VA Loma Linda Healthcare
System, Research (151)
11201 Benton Street
Loma Linda, CA 92357

8. PERFORMING ORGANIZATION REPORT NUMBER

9. SPONSORING / MONITORING AGENCY NAME(S) AND ADDRESS(ES)

U.S. Army Medical Research and
Materiel Command
Fort Detrick, MD 21702-5012

10. SPONSOR/MONITOR'S ACRONYM(S)

11. SPONSOR/MONITOR'S REPORT NUMBER(S)

12. DISTRIBUTION / AVAILABILITY STATEMENT

Approved for Public Release; Distribution Unlimited

13. SUPPLEMENTARY NOTES

14. ABSTRACT

We successfully identified two molecular targets among a handful candidates that may contribute to an escalated inner ear ototoxicity. One is the Duffy antigen receptor for chemokines (Darc), and the other is the transient receptor potential vanilloid 1 (TrpV1). Both receptors actively participate in the process of cochlear inflammation, a condition resulting from exposure to moderate and intense noise stimulation. During this reporting period, we continued research activities using electrophysiology, immunohistochemistry, and cochlear perfusion techniques to conduct proposed experiments. The effect of inflammation on drug- or noise-induced ototoxicity was further investigated, using the application of LPS or aminoglycosides. Acquired data were analyzed thoroughly and reported at conferences and prepared in manuscripts for peer-reviewed publication.

15. SUBJECT TERMS
Noise trauma, combat injury, otoprotection, aminoglycoside antibiotic, gentamicin, loop diuretic, furosemide, bacterial infection, LPS, ototoxicity, auditory function, hearing loss

16. SECURITY CLASSIFICATION OF:			**17. LIMITATION OF ABSTRACT**	**18. NUMBER OF PAGES**	**19a. NAME OF RESPONSIBLE PERSON**
a. REPORT	**b. ABSTRACT**	**c. THIS PAGE**			USAMRMC
Unclassified	Unclassified	Unclassified	Unclassified	34	**19b. TELEPHONE NUMBER** *(include area code)*

[SF298] Project Abstract

Background: Exposure to loud sounds causes temporary or permanent threshold shifts in auditory perception, with reversible or irreversible cellular damage in the cochlea. Noise trauma, or loud sound exposure, is particularly associated with military environments, especially when sustaining blast injuries. These injuries are frequently treated with aminoglycoside antibiotics that have broad-spectrum bactericidal activity for treating or preventing life-threatening infections. However, aminoglycosides are also toxic to the cochlea, leading to hearing loss and further degradation from pre-injury status. The combination of both prior noise trauma and aminoglycoside treatment can degrade auditory function greater than simple summation of the two insults. We have found that prior sound exposure enhances cochlear uptake of aminoglycosides, providing a mechanistic basis for the observed ototoxic synergy due to noise trauma and subsequent aminoglycoside treatment.

Objective/Hypothesis: The ultimate goal of this research is to prevent aminoglycoside-induced cochleotoxicity (as well as vestibulotoxicity and nephrotoxicity) that can severely debilitate the recovery of military personnel, including combatants and associated casualties to pre-injury effectiveness. In this proposal, we hypothesize that ***prior noise trauma induces synergistic ototoxicity with systemically-administered aminoglycosides by potentiating cochlear uptake of the drug.*** We also hypothesize that specific aminoglycoside-permeant cation channels directly facilitate noise trauma-enhanced uptake of aminoglycosides in the cochlea.

Specific Aims:

Aim 1: Determine the acoustic parameters that induce noise-enhanced aminoglycoside uptake in auditory sensory hair cells.

Aim 2: Determine if prior noise trauma modifies intra-cochlear trafficking of aminoglycosides.

Aim 3: Determine if aminoglycoside-permeant channels on the hair cell apical membrane contribute to aminoglycoside uptake by cochlear hair cells.

Aim 4: Determine if TRP channels on the basolateral membrane of cochlear hair cells also contribute to aminoglycoside uptake.

Study Design: In Aims 1, 3a and 4a, C57BL/6 mice, genetically-modified mice and Dunkin-Hartley guinea pigs will receive noise exposure followed by systemic aminoglycoside administration to determine the minimum and optimal acoustic paradigms that enhance hair cell uptake of aminoglycosides. Cochlear tissues will be examined by whole-mount preparation and confocal microscopy. In Aim 2 and 4b, cochlear perfusion will be performed with aminoglycosides administered either systemically or locally by scala tympani perfusion. In Aim 3b, noise-exposed organ of Corti will be prepared for scanning electron microscopy to correlate tip-link survival and drug uptake compared to control animals. In Aim 3c, cochlear explants will be prepared for MET blockade to determine if hair cells can take up aminoglycosides via TRPV4 and $P2X_2$ channels.

Relevance: Eliminating ototoxic synergy is not possible when prior loud or traumatic noise exposure is followed by treatment with aminoglycosides for blast, burns or penetrative injuries. The proposed research will test specific mechanisms to determine how noise trauma enhances aminoglycoside entry into cochlear hair cells to induce synergistic ototoxicity. This knowledge will enable the development of countermeasures to preserve auditory function during sequential and synergistic ototoxic insults in military environments.

Table of Contents

1. INTRODUCTION

Exposure to loud sounds causes temporary or permanent threshold shifts in auditory perception, with reversible or irreversible cellular damage in the cochlea. Noise trauma, or loud sound exposure, is particularly associated with military environments, especially when sustaining blast injuries. These injuries are frequently treated with aminoglycoside antibiotics that have broad-spectrum bactericidal activity for treating or preventing life-threatening infections. However, aminoglycosides are also toxic to the cochlea, leading to hearing loss and further degradation from pre-injury status. The combination of both prior noise trauma and aminoglycoside treatment can degrade auditory function greater than simple summation of the two insults. We have found that prior sound exposure enhances cochlear uptake of aminoglycosides, providing a mechanistic basis for the observed ototoxic synergy due to noise trauma and subsequent aminoglycoside treatment.

In the mammalian inner ear – the cochlea, the auditory sensory cells, particularly outer hair cells (OHCs), are more susceptible to aminoglycoside-induced cytotoxicity than other cochlear cells, particularly at the base of the cochlea most sensitive to higher frequency sound. Once these OHCs are lost, these sensory cells cannot be endogenously regenerated, leading to life-long hearing loss and deafness. Thus, extensive efforts are underway to ameliorate and prevent aminoglycoside-induced hair cell death. Under normal physiological condition, aminoglycosides can rapidly cross the blood-labyrinth barrier (BLB) into the cochlear tissues and fluids and enter OHCs through a number of conduits. The best-characterized conduit is permeation through the mechanoelectrical transduction (MET) channel. The MET channel is mechanically-gated by the extracellular, heterodimeric tip links between two stereocilia. Other mechanisms by which aminoglycosides can enter hair cells include endocytosis, and/or other aminoglycoside cation channels (*e.g.* TRP channels) expressed by hair cells besides the MET channel, such as TRPV4 on the apical membranes, or TRPA1 on the basolateral membranes, of OHCs.

The ultimate goal of this research is to prevent aminoglycoside-induced cochleotoxicity (as well as vestibulotoxicity and nephrotoxicity) that can severely debilitate the recovery of military personnel, including combatants and associated casualties to pre-injury effectiveness. In this project, we hypothesize that prior noise trauma induces synergistic ototoxicity with systemically-administered aminoglycosides by potentiating cochlear uptake of the drug. We also hypothesize that specific aminoglycoside-permeant cation channels directly facilitate noise trauma-enhanced uptake of aminoglycosides in the cochlea.

2. KEYWORDS

Noise trauma, combat injury, otoprotection, aminoglycoside antibiotic, bacterial infection, ototoxicity, auditory function, hearing loss

3. OVERALL PROJECT SUMMARY

What were the major goals of the project?

Aim 1: Determine the acoustic parameters that induce noise-enhanced aminoglycoside uptake in auditory sensory hair cells.

This is completed at OHSU.

Aim 2: Determine if prior noise trauma modifies intra-cochlear trafficking of aminoglycosides.

Aim 2a: Use cochlear perfusion techniques to determine the contribution of endolymph or perilymph trafficking of aminoglycosides to hair cells with prior noise exposure. GTTR will be administrated either systemically or by scala tympani infusion to the animal.

This is completed at OHSU.

Aim 3: Determine if aminoglycoside-permeant channels on the hair cell apical membrane contribute to aminoglycoside uptake by cochlear hair cells.

Aim 3a: Determine if prior noise trauma enhances drug uptake in hair cells.

This is completed at Loma Linda.

Aim 3b: Examine tip-link integrity in noise-exposed rodents by scanning electron microscopy.

This is completed at Loma Linda.

Aim 3c: Confirm that hair cell $P2X_2$ and TRPV4 channels are aminoglycoside-permeant.

This is completed at Loma Linda.

Aim 4: Determine if TRP channels on the basolateral membrane of cochlear hair cells also contribute to aminoglycoside uptake.

Aim 4a: Determine if noise enhances drug uptake in TrpA1 or TrpV1 mice.

This is completed at Loma Linda.

Aim 4b: Verify that scala tympani perfusion of TRPA1 or TRPV1 antagonists in noise-exposed guinea pigs inhibit noise-enhanced uptake of GTTR.

This is partially completed at Loma Linda.

What was accomplished under these goals?

1) Major activities

During this reporting period, we continued research activities using electrophysiology, immunohistochemistry, and cochlear perfusion techniques to conduct proposed experiments in this project. New members joined the lab and some senior lab members left. Trainings on essential techniques and protocols were provided upon the transitions. The effect of inflammation on drug- or noise-induced ototoxicity was further investigated, using the application of noise, LPS or aminoglycosides. Acquired data were analyzed thoroughly and reported at conferences and prepared in manuscripts for peer-reviewed publication.

2) Specific objectives

a) We continued to host the mouse cohorts which are essential materials for the project. Major colonies include *TrpV1* mice (#3770), *Darc* mice, wildtype *CBA/CaJ* mice (#0654) and wildtype *C57BL/6* mice (#0664) in the animal facility (VMU) at Loma Linda VA Healthcare System. For mice that are available from accredited vendors (*e.g.* Jackson Laboratory, Bar Harbor, ME), breeding pairs were periodically purchased to keep the cohorts genetically consistent with the original source.

b) We investigated the effect of intratympanic LPS on cochlear uptake of ototoxic aminoglycosides, in both wildtype mice and in *TrpV1* mice. We studied the correlation between modulated drug uptake and inflammatory events, including the morphology and infiltration of cochlear macrophages and the variation of immune active cytokines' variation.

c) We continued to monitor a small *TrpV1* mouse cohort (as well as a *Darc* mouse cohort) as they are getting older, to reveal the effect of the mutant allele on the systemic aging process.

d) We investigated the dose-dependent effect of gentamicin and furosemide in combination on producing cochlear damage, by 1) characterizing the residual hearing function, using both electrophysiologic approach (ABR) and acoustic approach (DPOAE), 2) distinguishing the morphology of outer and inner hair cells, and ribbon synapses at various cochlear locations, and at multiple posttreatment time points, and 3) determination of the synaptic variation in number, and in morphological distribution.

4. KEY RESEARCH ACCOMPLISHMENTS

a) Combining loop diuretics to aminoglycoside treatment is an effective approach for accelerating ototoxic damage, especially, in mice, which results in immediate cochlear trauma (Hirose and Sato, 2011; Taylor *et al.*, 2008). In this simplified version of a mouse ototoxicity model, the addition of loop diuretics, such as furosemide, disrupts the blood labyrinth barrier thereby greatly elevating the concentration of aminoglycosides, such as gentamicin, in the cochlea (Ding *et al.*, 2016; Taylor *et al.*, 2008). Furosemide, by itself, is not considered directly damaging to the inner-ear components including hair cells (HCs), ribbon synapses or spiral ganglion neurons (SGNs) (Rybak, 1993). In the present study, the dose-dependent effect of gentamicin and furosemide (G/F) in combination was investigated to: 1) characterize the residual hearing function, 2) distinguish the morphology of OHCs and IHCs, and ribbon synapses at various cochlear locations, and 3) determine whether there is a change in the number, or the distribution, of synaptic ribbons.

Seven days after the one-time G/F treatment, synaptic ribbons that were identified by the anti-CtBP2 labeling exhibited various degrees of morphological change. On the *xy* plane at the cochlear location equivalent to 12 kHz (Müller *et al.*, 2005), the ribbon distribution appeared normal for some low-dose G/F treatments, demonstrated by a vacant zone basally located to the IHC nuclei, without a reduction in the number of ribbons, *i.e.*, ribbon density, as illustrated by the micrographs of Figs. 1A1-A4. Among them, Figs. 1A2-A4 are the confocal images reconstructed in the *yz* plane from three adjacent IHCs. Similar to our previous findings in healthy control cochleae, the size of ribbons near the nuclei was relatively small, while those located at the IHC basal pole were larger (Edderkaoui *et al.*, 2018). In addition, it is noteworthy that with the mounting technique used, the IHCs from the apex and the middle coils of the cochlea generally orientate in parallel to the cover slide, which allowed a convenient quantifying of the distance of individual ribbons to the nucleus along the *y* axis, *i.e.*, the main axis of the IHC. Thus, a shape of normal distribution along the main axis was typically anticipated, as indicated in Fig. 1A5. Yet, under most G/F treatment conditions, a certain distribution disorder was observed, for example, in Figs. 1B1-B5, manifested by some ribbons being shifted toward the IHC nucleus without a reduction in the number of ribbons. In addition, the "nucleus-ward or upward" shift appeared predominantly toward the pillar side of the IHC as shown on the left side of Figs. 1B2 and 1B4. The axial gradient based on the ribbon size was also disturbed. In the extreme ototoxic scenario, the ribbon numbers did decline after some high-dose G/F treatments, with extensive upward shift of the ribbons as illustrated in Fig. 1C2, and enlarged ribbons in many cases as demonstrated in Fig. 1C1.

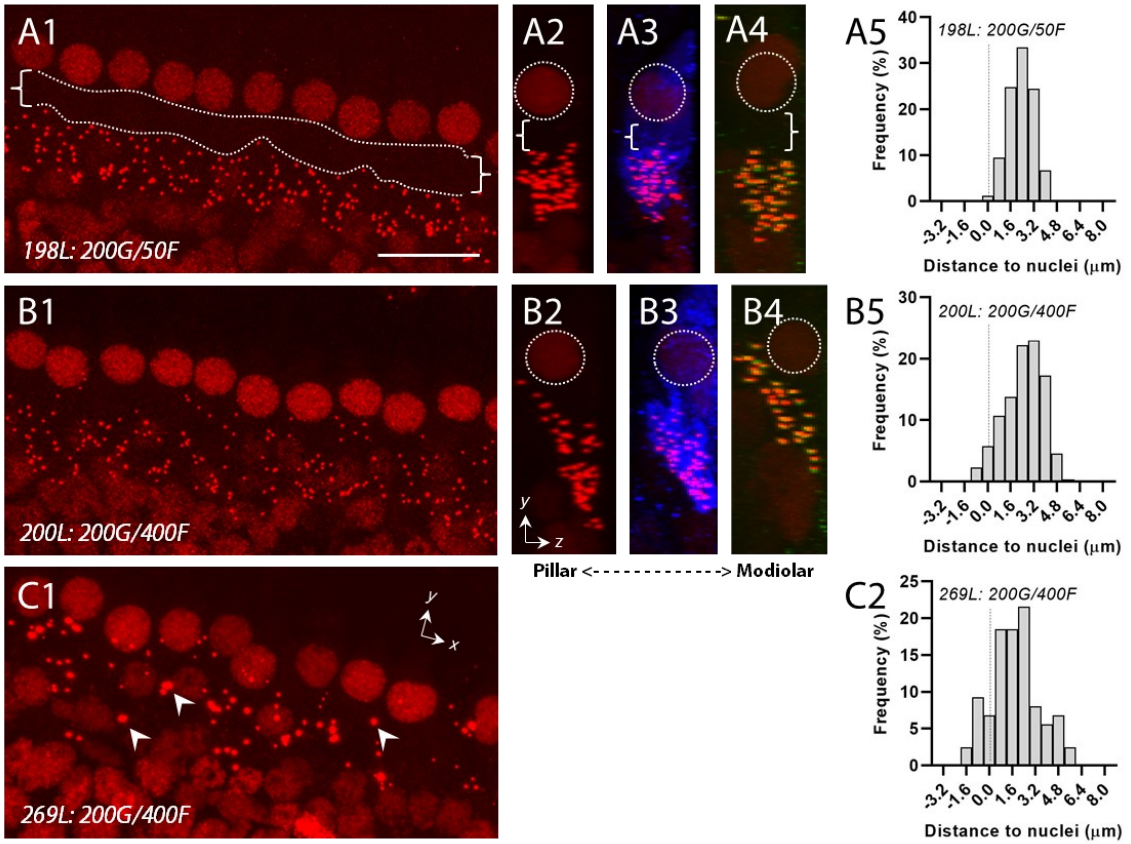

Figure 1. Alteration of synaptic ribbons after G/F treatment. A: In the apical and middle cochlear locations free of OHC damage, low-dose G/F treatment might not induce any visible change in CtBP2-labeled synaptic ribbons (red puncta), showing a characteristic vacant zone depicted by brackets and dotted lines basal to the IHC nucleus in the xy plane (A1). Error bar=20 μm. Reconstructed images in the yz plane from three adjacent IHCs exhibited the distribution of ribbons along the pillar-modiolar axis (A2), with identification of the cytoplasm of the IHC by anti-Myo7a immunolabeling (A3, blue), and paired postsynaptic AMPA receptors by anti-GluR2 immunolabeling (A4, green). A semi-normal distribution of the ribbon along the main cell axis was often observed (A5). B1-4: Seven days after G/F treatment, at cochlear locations free of OHC damage, a pillar-side upward shift of synaptic ribbons was often seen without a reduction in ribbon number. B5: ribbon distribution along the main cell axis was skewed to the nucleus. C1: With severe cochlear damage induced by G/F treatment, the ribbon density could be drastically reduced and many individual ribbons enlarged (arrowhead), and again, often exhibiting an upward shift (C2).

b) Combined gentamicin and furosemide treatment resulted functional deficit in outer hair cells. Average DPOAE responses in the fixed dose of gentamicin groups, to 55-dB SPL primary tones, from representative ears, comparing G/F pretreatment (blue) and 7-day posttreatment (red) conditions is shown in Figs. 2A-D. Gentamicin alone (200 mg/kg) did not result in any DPOAE deficit (Fig. 2A; $F(1,656)=0.452$, $p=0.502$), while OHC injury preferably occurred at the high-frequency region, and the injury expanded to lower frequency regions as the dose of furosemide increased from 50 mg/kg to 400 mg/kg (Figs. 2B-D), suggesting the overall ototoxic severity escalated. This dose-dependent ototoxic principle could also be observed in individual animals. However, note the large, red shaded range of standard deviation of

average DPOAE responses at 7-day after G/F-treatment, *e.g.*, Fig. 2D, which indicated the ototoxic OHC injury was highly variable, similar to the aforementioned inter-animal variability observed in ABR thresholds. A manuscript has been prepared to summarize these general findings in mice treated with G/F combination. The manuscript is attached by the end of this progress report.

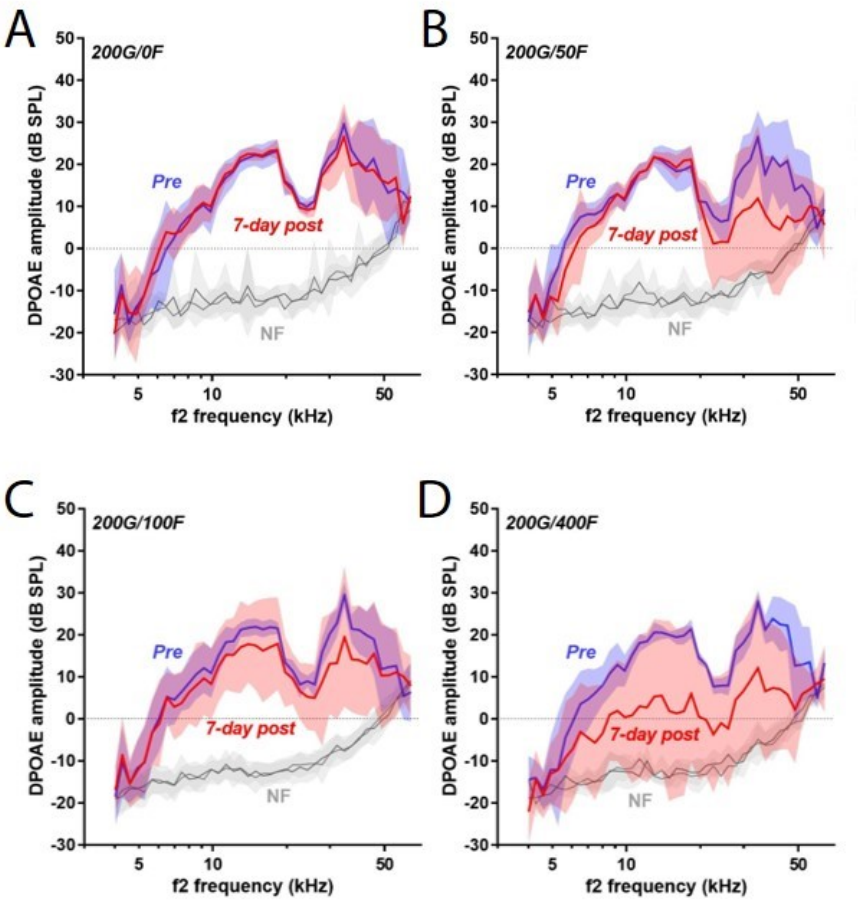

Figure 2: DPOAE revealed OHC damage from G/F treatment in individual mice. A-D: In the fixed dose of gentamicin groups, the introduction of furosemide at varied doses generally caused a dose-dependent DPOAE deficit in the cochlea. Sound levels of the primary tones were equal at L1=L2=55 dB SPL, f2/f1=1.25. NF=noise floor. Shaded area depicted boundaries indicate standard deviation.

c) It is known that intensive noise exposure elevates cochlear immune activities, partly manifested by the increased number of tissue specific macrophages in the cochlea. Accordingly, we rationalized that the prior noise trauma-induced cochlear immune activity includes TRPV1 channel activation which subsequently enhances aminoglycoside ototoxicity. To test above hypothesis, we induced reliable cochlear inflammation by systemic endotoxemia. In these mice, we observed increased expression of TrpV1 in the cochlea and increased uptake of circulating aminoglycosides (GTTR as a tracer) by hair cells (Jiang, Li *et al.*, 2019).

Alternatively, we also induced reliable cochlear inflammation by topical lipopolysaccharide (LPS) treatment, and investigated cochlear macrophages by Iba1 labeling.

In recent years, Iba1 antibody has been increasingly used in hearing research labs as a cell marker to identify tissue macrophages/microglia. After LPS inoculation, we observed increased number of Iba1+ cells in many cochlear locations, including the spiral ligament, the basilar membrane, the spiral limbus and the spiral lamina, but not in the stria vascularis (Chai *et al.*, 2020).

Thus, both noise and bacterial exposure induce cochlear inflammation, and subsequently enhance aminoglycoside ototoxicity. Here, we also question if aminoglycoside treatment itself activates cochlear immune cells, by using tandem intraperitoneal gentamicin and loop diuretic furosemide (G/F) to challenge the inner ear tissue. We did observe increased Iba1-positive activities along the basilar membrane, specially at the spiral laminar, 3-day and 7-day after the G/F treatment (Fig. 3). The Iba1+ activity appears more prominent on 3-day posttreatment compared to 7-day. Although higher gentamicin dose (400 mg) resulted in hair cell loss, but not necessarily more Iba1+ activity.

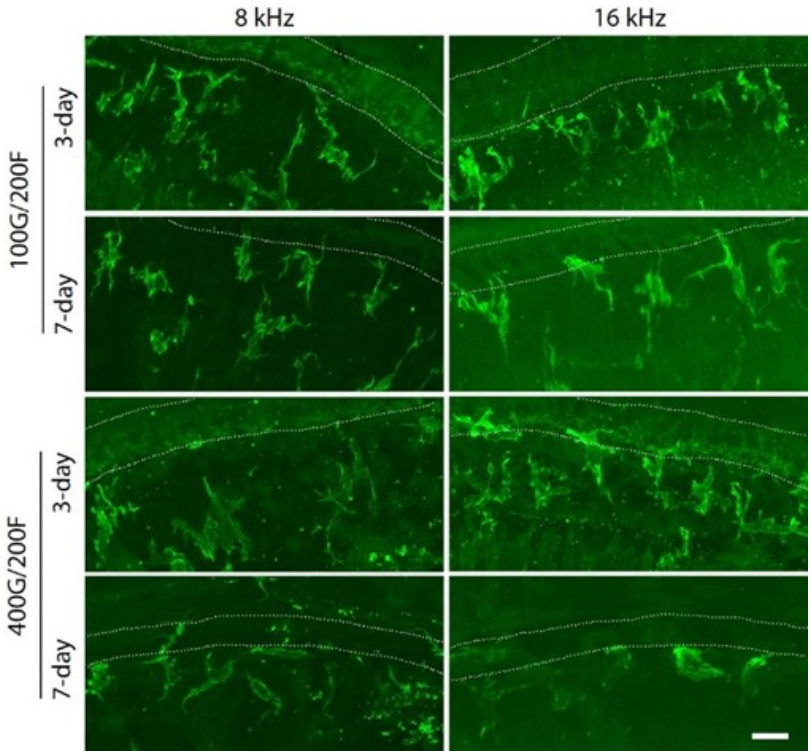

Figure 3. Induction of cochlear macrophages after combined treatment of gentamicin and furosemide. Three days or seven days after the combined treatment using 100 mg/kg gentamicin and 200 mg/kg furosemide (top panels), or 400 mg/kg and 200 mg/kg furosemide (bottom panels), macrophages or microglia cells were immunolabeled by anti-Iba1 antibodies with green fluorescence. Micrographs indicated elevated Iba1+ activity at the cochlear locations equivalent to 8 and 16 kHz in the spiral laminar. Dotted lines depict the location of inner hair cells, and scale bar=20 µm.

d) In the past a few years, we have gained increasing understanding on external factors that agitate the inner ear immune homeostasis, including acoustic overexposure, bacterial inoculation, and aminoglycoside application. All our prior experiments in the project were conducted in *C57BL/6 (BL6)* mice. We already knew that different wildtype mouse strains

exhibited varied susceptibility to aminoglycoside ototoxicity, as well as to noise challenge. For instance, *BL6* mice are frequently used as the ototoxicity mouse model, while *CBA/CaJ (CBA)* mice are suggested in other hearing-related studies, given that *BL6* strain harbors the premature and age-related hearing loss gene. Thus, the mouse strain effect on the activation of cochlear immune response is an inevitable scientific question. We performed intratympanic (*i.t.*) injection of LPS in both *BL6* and *CBA* mice, and documented the morphological response of Iba1-positive macrophages in the cochlea, specifically in the organ of Corti, along the basilar membrane. In sum, *i.t.* LPS inoculation activated Iba1+ macrophages in both wildtype strains, while *BL6* mice exhibited higher responsive features, including the increase of macrophage numbers and extensive arborization. The difference between two strains appeared more significant in the basal region of the cochlea. The selection of *BL6* mice in the current project was a proper decision to demonstrate underlying ototoxic and immunological mechanisms.

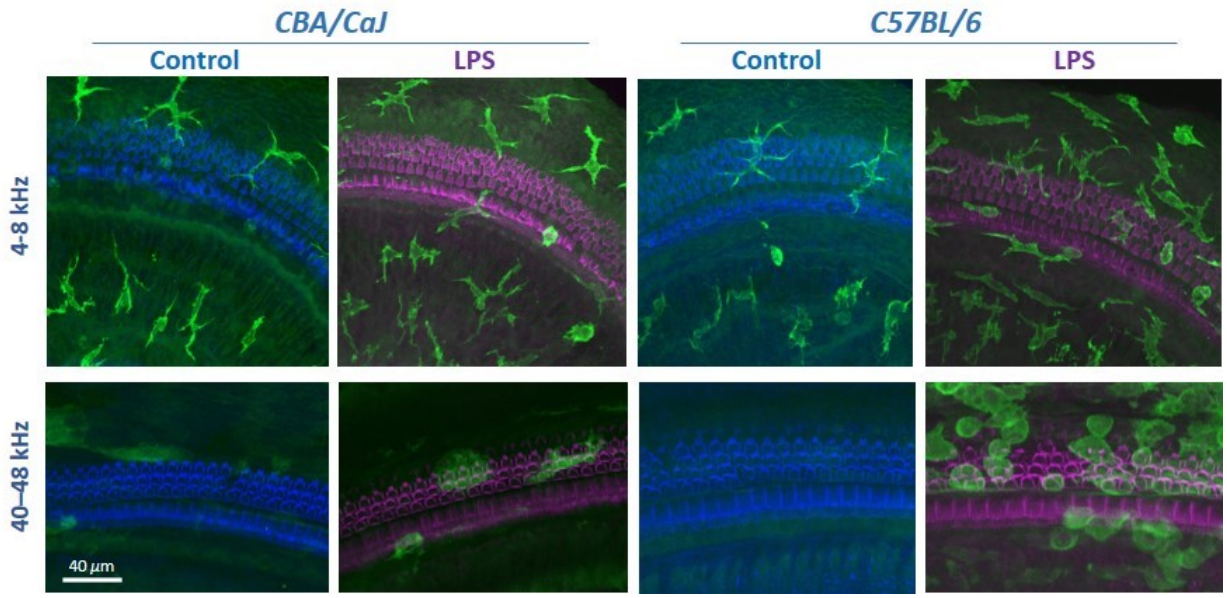

Figure 4. Induction of cochlear macrophages after intratympanic LPS treatment. Two days after the LPS treatment (1 mg/ml, 10 μl), micrographs indicated elevated Iba1+ activity at both the apical and basal cochlear locations. The elevated macrophage activity was more prominent in C57BL/6 mice compared to CBA/CaJ mice. Scale bar=40 μm.

5. CONCLUSION

Cochlear inflammation has gradually becoming a major research topic in recent years in auditory neuroscience. It is first known that intensive noise exposure elevates cochlear immune activities, manifested by increased number of tissue specific macrophages and elevated cytokine levels in the cochlea. In addition, we recently found that aminoglycosides also trigger cochlear immune response without other extrinsic inflammatory triggers. This finding raised the clinical

significance of this line of research, given that aminoglycoside antibiotics are often prescribed to patients with systemic or local infection to suppress a potential or ongoing bacterial presence. The exact role of these cochlear macrophages and their elevated activities is not totally clear. It is known that the function of tissue macrophages is multifaced. We studied the event sequence upon aminoglycoside-induced cochlear damage, including hair cell loss, synaptic damage and macrophage behavior. The recruitment or proliferation of cochlear macrophages appeared as a prelude to hair cell loss, and definitely occurred ahead of synaptic damage. These findings suggest that cochlear macrophages, at least the ones located in the spiral laminar, likely underpin a protective mechanism to the neuronal elements in the cochlea that is essential for a reliable signal transmission, and certainly warrant further investigation.

Over the project period of XW81XWH-14-1-0006, we have successfully identified two molecular targets among a handful candidates that may contribute to an escalated inner ear ototoxicity. One is the Duffy antigen receptor for chemokines (Darc), and the other is the transient receptor potential vanilloid 1 (TrpV1). Understanding their presence in the untreated cochlea and modulation in the inflammatory cochlea are essential in the development of countermeasures to prevent cochlear damage by variety of insults, including but not limited to acoustic overexposure and drug-induced ototoxicity.

6. PUBLICATIONS, ABSTRACTS AND PRESENTATIONS

Peer reviewed publication

Liana Sargsyan, Alisa P. Hetrick, Marjorie R. Leek, Glen K. Martin, Hongzhe Li (Submitted to NeuroToxicology), Effects of combined gentamicin and furosemide treatment on cochlear ribbon synapses.

Yongchuan Chai, Weiwei He, Weiqiang Yang, Alisa P. Hetrick, Jessica Gonzalez, Liana Sargsyan, Hao Wu, Timothy T.K. Jung, Hongzhe Li (Submitted to Laryngoscope), Intratympanic injection of lipopolysaccharide elevates systemic gentamicin uptake in the cochlea

Conference abstracts, papers and podium presentations

Yongchuan Chai, Alisa Hetrick, Liana Sargsyan, Weiwei He, Timothy Jung, Hao Wu, Hongzhe Li (2020), “Intratympanic Lipopolysaccharide Induces Inflammatory Responses and Elevates Systemic Gentamicin Uptake in the Cochlea”, 43rd Midwinter Research Meeting in Otolaryngology, San Jose, CA.

Liana Sargsyan, Alisa Hetrick, Yongchuan Chai, Hongzhe Li (2020), "The Response of Cochlear Microglia-Like Cells to Ototoxic Challenge in Different Strains of Wildtype Mice", 43rd Midwinter Research Meeting in Otolaryngology, San Jose, CA.

7. INVENTIONS, PATENTS AND LICENSES

Nothing to report.

8. REPORTABLE OUTCOMES

What opportunities for training and professional development has the project provided?

This research project provided opportunities for people with interest and motivation in biomedical research, including college students and international physicians. Liana Sargsyan, a European trained physician, and Weiqiang Yang, a full feathered doctor from Shenzhen, are both specialized in otology and worked in the PI's lab during the reporting period. They have both contributed to the project, accrued hands-on experience in cochlear dissection, and image acquisition *etc*. This experience will certainly provide positive impact on their upcoming career advancement.

What individuals have worked on the project?

Name: Hongzhe Li, PhD
Project Role: PI
Nearest person month worked: 6.0
Contribution to Project: Dr. Li has performed work in experimental design, staff training, tissue harvest and processing, confocal imaging, image acquisition and quantification, data analysis, documents, protocols, reports and manuscript preparation.

Name: Alisa Hetrick, BSc
Project Role: Research Technician
Nearest person month worked: 1.0
Contribution to Project: Ms. Hetrick has performed work in ABR and DPOAE recordings, noise and aminoglycoside exposures, and managed mouse cohort with genotyping

procedures. She also assisted in acquiring lab equipment and consumables, and protocol development.

Name: Jessica Gonzalez, BSc
Project Role: Research Technician
Nearest person month worked: 5.0
Contribution to Project: Ms. Gonzalez has performed work in ABR and DPOAE recordings, noise and aminoglycoside exposures, and managed mouse cohort. She also assisted in acquiring lab equipment and consumables, and data analysis.

Name: Liana Sargsyan, MSc
Project Role: Research Associate
Nearest person month worked: 12.0
Contribution to Project: Ms. Sargsyan has performed work in animal treatment with aminoglycosides, cochlear microdissection, confocal microscopy, data analysis, and conference presentation, and manuscript preparation.

Name: Weiqiang Yang, MD
Project Role: Research Associate
Nearest person month worked: 4.0
Contribution to Project: Dr. Yang has performed work of cochlear perfusion and intratympanic injections in mice, as well as cochlear microdissection, immunohistochemistry, confocal microscopy and data analysis.

How were the results disseminated to communities of interest?

Part of the content in this report has been presented at the following conferences

- Midwinter meeting of Association for Research in Otolaryngology (2020), San Jose, CA.

9. OTHER ACHIEVEMENTS

a) Other general lab activities included personal recruitment and lab orientation, lab safety and compliance training, equipment acquisition and setup, and protocol selection or development *etc*.

b) During the last quarter of this annual reporting period, we did experience delays due to the Covid-19 pandemic. The Governor of the State of California issued an order in mid-March asking all non-essential worker to remain at home and practice social distancing. In seeking to comply with the order, my laboratory staff had been confined to essential duties such as animal care with reduced mouse cohorts, and the daily routine of conducting experiments had been significantly delayed. We took these precautions very seriously as my laboratory is located in a Veterans Affairs Medical Center, and so the immediate concern is for the welfare of the patient population. In response to the circumstance, the PI and senior lab members switched their focus onto data analysis and manuscript preparation.

10. REFERENCES

1. Ding D, Liu H, Qi W, Jiang H, Li Y, Wu X, et al. Ototoxic effects and mechanisms of loop diuretics. J Otol. 2016;11(4):145-56.

2. Edderkaoui B, Sargsyan L, Hetrick A, Li H. Deficiency of Duffy Antigen Receptor for Chemokines Ameliorated Cochlear Damage From Noise Exposure. Frontiers in Molecular Neuroscience. 2018;11(173).

3. Hirose K, Sato E. Comparative analysis of combination kanamycin-furosemide versus kanamycin alone in the mouse cochlea. Hear Res. 2011;272(1-2):108-16.

4. Jiang M, Li H, Johnson A, Karasawa T, Zhang Y, Meier WB, et al. Inflammation up-regulates cochlear expression of TRPV1 to potentiate drug-induced hearing loss. Sci Adv. 2019;5(7):eaaw1836.

5. Muller M, von Hunerbein K, Hoidis S, Smolders JW. A physiological place-frequency map of the cochlea in the CBA/J mouse. Hear Res. 2005;202(1-2):63-73.

6. Rybak LP. Ototoxicity of loop diuretics. Otolaryngol Clin North Am. 1993;26(5):829-44.

7. Taylor RR, Nevill G, Forge A. Rapid hair cell loss: a mouse model for cochlear lesions. J Assoc Res Otolaryngol. 2008;9(1):44-64.

11. APPENDICES

A manuscript submitted to the journal of NeuroToxicology.

Effects of combined gentamicin and furosemide treatment on cochlear ribbon synapses

Liana Sargsyan[1], Alisa Hetrick[1], Marjorie R. Leek[1,2], Glen K Martin[1,2], Hongzhe Li[1,2,*]

1. *Research Service, VA Loma Linda Healthcare System, CA 92357, USA*
2. *Department of Otolaryngology - Head and Neck Surgery, Loma Linda University Health, Loma Linda, CA 92354, USA*

*Corresponding author: Hongzhe Li, PhD

Research Service (151), VA Loma Linda Healthcare System, 11201 Benton Street, Loma Linda, CA 92357, USA. *E-mail:* Hongzhe.Li@va.gov. *Tel:* 1(909)825-7084 Ext 2816. *Fax:* 1(909)796-4508

Running Title: Synaptic damage by gentamicin and furosemide

Keywords: Aminoglycosides, loop diuretics, cochlea, hair cells, synaptopathy, hidden hearing loss.

Abstract

It is well-established that aminoglycoside antibiotics are ototoxic, and the toxicity can be drastically enhanced by the addition of loop diuretics, resulting in rapid irreversible hair cell damage. Recent research also indicated that the combined treatment could lead to the loss of spiral ganglion neurons prior to the loss of hair cells, reminiscent of the disease termed as auditory neuropathy (AN). Using both electrophysiologic and morphological approaches, we investigated whether this treatment affected the cochlea, at the region of ribbon synapses consequently resulting in auditory synaptopathy representing a unique form of AN. A series of varied gentamicin and furosemide doses were applied to *C57BL/6* mice, and auditory brainstem responses (ABR) and distortion product otoacoustic emissions (DPOAE) were measured to assess ototoxic damage within the cochlea. In brief, the treatment effectively induced cochlear damage and promoted a certain reorganization of synaptic ribbons, while a reduction of ribbon density only occurred after a substantial loss of outer hair cells. In addition, both the ABR wave I amplitude and the ribbon density were elevated in many treatment conditions, but a correlation between the two events was insignificant for individual cochleae. In sum, combined gentamicin and furosemide treatment, at titrated doses below those that produce hair cell damage, typically triggers synaptic plasticity rather than a permanent synaptic loss.

1. Introduction

Cochlear synaptopathy is manifested by a loss of synaptic connections between cochlear inner hair cells (IHCs) and their auditory nerve fiber (ANF) terminals that results in a delayed degeneration of spiral ganglion neurons (SGNs) and their central axonal projections (Moser and Starr, 2016). With noise overexposure, it is possible to create animal models exhibiting a selective and permanent synaptic loss with relatively intact hair cells (HCs) in a phenomenon termed hidden hearing loss (HHL), which has been studied extensively by Kujawa and Liberman (Kujawa and Liberman, 2009, 2015; Liberman and Kujawa, 2017). In the meantime, it is less clear if the HHL-type of synaptopathy can be induced by other cochlear insults, which often result in considerable plasticity in terms of affecting hair-cell synaptic densities. Using moderate dosing, aminoglycoside antibiotics can produce a specific SGN death without much damage to HCs in genetically modified mice (Oishi et al., 2015), thus, suggesting the likelihood of cochlear synaptopathy (Jiang et al., 2017). A chemical model of the acoustic synaptopathy in mice is certainly welcomed by the research community to simplify the

preparation procedure, while taking advantage of the readily available manipulation of the murine genome. Yet, to date, a convincing synaptopathy indicating HHL has not been demonstrated *in vivo* in mice by any known aminoglycoside treatment (Hong et al., 2018; Liu et al., 2015; Liu et al., 2013).

Prior to the raised attention on synaptopathy, cochlear insults, regardless of being produced by acoustic overstimulation or aging, were believed to first target sensory elements in the mouse cochlea, followed by their associated neural components such as the SGNs (Willott et al., 1998). Moreover, the resulting damage appeared to be more biased toward the sensitive outer hair cells (OHCs) on the sensory epithelium (Spongr et al., 1997; Willott et al., 1998). Intuitively, these outcomes were not what was expected to occur in an ideal synaptopathy animal model, in which a considerable reduction of the synaptic density with intact HC survival assessed by morphological or electrophysiological approaches, is ordinarily expected. Intriguingly, Ruan et al. (Ruan et al., 2014) reported that a single intraperitoneal injection of gentamicin, assisted by a loop diuretic, furosemide, induced a SGN loss that could occur before damage to HCs, especially, IHCs, which is reminiscent of the disease termed auditory neuropathy (AN). Here, we asked if the ribbon synapse of the IHC could be compromised ahead of HC loss, regardless of the condition of the SGNs. As aforementioned, this would be significant, because it would replicate the HHL that is typically observed with noise overexposure or in certain aging animal models. Mechanistically, independent synaptic damage, *i.e.*, HHL, is possible because aminoglycosides are capable of inducing the excitotoxic type of injury at the synaptic level, which is considered to be a major underlying mechanism for noise-induced HHL (Basile et al., 1996; Liberman and Kujawa, 2017; Segal et al., 1999).

Combining loop diuretics to aminoglycoside treatment is an effective approach for accelerating ototoxic damage, especially, in mice, which results in immediate cochlear trauma (Hirose and Sato, 2011; Taylor et al., 2008). In this simplified version of a mouse ototoxicity model, the addition of loop diuretics, such as furosemide, disrupts the blood labyrinth barrier thereby greatly elevating the concentration of aminoglycosides, such as gentamicin, in the cochlea (Ding et al., 2016; Taylor et al., 2008). Furosemide, by itself, is not considered directly damaging to the inner-ear components including HCs, ribbon synapses or SGNs (Rybak, 1993). In the present study, the dose-dependent effect of gentamicin and furosemide (G/F) in combination was investigated to: 1) characterize the residual hearing function, 2) distinguish the morphology of OHCs and IHCs, and ribbon synapses at

various cochlear locations, and 3) determine whether there is a change in the number, or the distribution, of synaptic ribbons.

The G/F combination treatment is also frequently used to induce cochlear HC loss prior to testing a specific strategy for regenerating HCs (Izumikawa et al., 2005). Excessive damage toward other cochlear components including the ribbon synapse is considered an unfavorable ototoxic event and certainly complicates the assessment of a HC's regeneration capacity. Thus, whether G/F treatment could induce an HHL-type of synaptopathy is an important scientific question, and valuable to the research community with either outcome. We, therefore, examined in detail the effects on the mouse cochlea of this treatment combination using a series of varied doses of G/F.

2. Methods

2.1 Mice and gentamicin/furosemide (G/F) treatment

C57BL/6 (JAX stock #0664) wild-type mice of both sexes, between 6-8 wk of age, were included in the present study. Animals were housed in a Specific Pathogen Free-modified room. Experimental animals were injected intraperitoneally (*i.p.*) with a single dose of gentamicin (Sigma-Aldrich, G1264, Lot #SLBG7734V) followed within 30 min by furosemide (Fresenius Kabi, Germany). Age-matched mice without any ototoxic treatment served as controls. The dose combination was either a fixed gentamicin injection at 200 mg/kg body weight, with varied furosemide doses (50, 100, 200, 400 mg/kg), or a fixed furosemide dose (200 mg/kg) with varied gentamicin injections (25, 50, 100, 200, 400 mg/kg), as illustrated in Supplemental Fig. 1. The majority of mice underwent distortion product otoacoustic emissions (DPOAE) and auditory brainstem response (ABR) tests prior to, and at several posttreatment time points, *i.e.*, primarily at day 3 and day 7. Seven days after treatment, mice were terminated and cochlear tissues harvested for morphological examination. Cochlear samples from a subset of mice were collected 2 days after the G/F treatment. Data reported here were collected from a total of 60 mice. Only three mice did not survive the treatment, including two, which were treated with 400 mg/kg gentamicin and 200 mg/kg furosemide (400G/200F) doses. All animal work was carried out using protocols approved by the Institutional Animal Care and Use Committee of the Jerry L. Pettis VA Medical Center, Loma Linda, CA. Animal-use procedures conformed with federal regulations regarding personnel, supervision, record keeping, and veterinary care.

105 *2.2 ABR and DPOAE measurement*

106 Individual anesthetized mice (ketamine 65 mg/kg/xylazine 13 mg/kg, *i.p.*) were stimulated with a
107 closed tube sound-delivery system sealed into the outer ear canal. ABRs to tone-burst stimuli (5-ms
108 duration, 1-ms rise/fall times) at 4, 8, 12, 16, 24 and 32 kHz, at 5-dB steps, were recorded using a
109 Tucker-Davis Technologies (TDT) System 3 (Alachua, FL, USA). In particular, thresholds and wave I
110 peak-to-peak amplitudes were determined. A full range of input/output (I/O) functions of wave I
111 amplitudes was typically recorded in response to 12-kHz tone-bursts.

112 $2f_1$-f_2 DPOAEs were measured to non-invasively assess OHC function (Jimenez et al., 1999).
113 Briefly, the f_1 and f_2 primary tones were generated by a dual-channel synthesizer (Hewlett Packard
114 Model 3326A) and attenuated under the control of in-house customized software. The f_1 and f_2 primary
115 tones (f_2/f_1=1.25) were mixed acoustically and delivered to two separate ear-speakers (Tandy Corp,
116 Fort Worth, TX) to avoid artifactual distortion. Ear-canal sound pressure levels were measured by an
117 emissions microphone assembly (Etymotic Research, ER-10B+, Elk Grove Village, IL), embedded in
118 the probe. Sound levels were sampled, synchronously averaged and Fourier analyzed for f_2's ranging
119 from 4.0-64.0 kHz in 0.1-ocatave steps. Corresponding noise floors (NFs) were computed by
120 averaging the levels of the ear-canal sound pressure for five frequency bins above and below the $2f_1$-f_2
121 frequency bin. Primary tones were presented at L_1=L_2=55 dB SPL.

122 *2.3 Tissue-processing, image acquisition and processing*

123 Cochlear samples were immersion-fixed overnight in 4% paraformaldehyde (pH 7.4), followed by
124 EDTA (10%, pH 7.4) decalcification at room temperature (RT). To prepare the cochlear whole-
125 mounts, the membranous labyrinth of the cochlea was micro-dissected under a dissecting microscope
126 to remove the softened otic capsule, stria vascularis, Reissner's membrane, and tectorial membrane.
127 After further immersion-fixation in 4% paraformaldehyde, specimens were permeabilized in 1%
128 Triton-X solution for 1 h at RT. Then, specimens were incubated at 37°C overnight with primary
129 antibodies including monoclonal mouse anti-CtBP2 IgG1 (612044, BD Biosciences, 1:200),
130 monoclonal mouse anti-GluR2 IgG2a (MAB397; Millipore; 1:1000), and/or polyclonal rabbit anti-
131 Myo7a (PA-936, Thermo Fisher, 1:200). After rinsing, the specimens were incubated with the Alexa
132 Fluor 594- and 568-conjugated secondary antibodies at 1:1000 at 37°C for 1 h in the dark. Some
133 specimens were also incubated with Alexa Fluor 488 phalloidin at a 1:1000 at RT for 20 min in the

dark. After the final wash, the modiolus was removed from the tissue and the epithelia were divided into segments and mounted on slides with the anti-fade fluorescence mounting media VectaShield (Vector Labs, Burlingame, CA) under uniform 60X magnification. Immunolabeled images were acquired using a laser confocal microscope (Fluoview FV3000, Olympus Corp.).

Data were analyzed using Prism (GraphPad Software, La Jolla, CA, USA) software for Windows. Statistical methods included a 2-way ANOVA with Sidak multiple comparisons, and unpaired t-tests with Welch's correction. All tests were two-tailed, and a p value of <0.05 was considered statistically significant.

3. Results

3.1 Gentamicin/furosemide dose response and inter-animal ototoxicity variation

To test whether a single combined dose of ototoxic treatment influenced the ribbon synapse in mouse models of acquired sensorineural hearing loss, we tested *C57BL/6* wild-type mice as an established animal model of HC loss.

In *C57BL/6* mice, when gentamicin dosage was fixed at 200 mg/kg, a dose effect of furosemide was evident in terms of group ABR thresholds measured at 3 and 7 days after G/F treatment, from 0 to 400 mg/kg as illustrated in Figs. 1A-D. For lower furosemide dosages including 50 (200G/50F) and 100 (200G/100F) mg/kg, as shown in Figs 1B and 1C, respectively, average ABR thresholds were elevated at the higher tested frequencies of 24 and 32 kHz. The elevation was statistically significant for the 200G/100F treatment (2-way ANOVA, 7-day *vs.* pre, $F(1,60)=8.31$, $p=0.0055$), and barely insignificant for the 200G/50F treatment (2-way ANOVA, 7-day *vs.* pre, $F(1,60)=3.22$, $p=0.078$). For the higher 400 mg/kg furosemide dosage (200G/400F) illustrated in Fig. 1D, the average ABR thresholds increased across the entire frequency-test range (2-way ANOVA, 7-day *vs.* pre, $F(1,60)=79.9$, $p<0.0001$), indicating severe cochlear injury. Although a dose response of furosemide did exist from group data as indicated in Figs. 1A-D, it is noteworthy that the large inter-animal variation made it impossible to reversely predict G/F dose based on individual ABR thresholds. For instance, an ear with 200G/400F treatment (purple lines in Figs. 1E and 1F) could present normal ABR thresholds, while an ear with 200G/50F treatment (green line in Figs. 1E and 1F) presented undetectable ABR thresholds at higher frequencies. When undetectable, a threshold value of 95 dB

was assigned for group-averaging purposes. ABR thresholds measured from other G/F dose combinations are illustrated in Suppl. Fig. 2.

DPOAEs were also measured in most G/F-treated *C57BL/6* mice, thus, providing a more sensitive and reliable injury assessment in individual animals, while the assessment was restricted at the level of the OHCs. DPOAE responses to 55-dB SPL primary tones, from representative ears, comparing G/F pretreatment (blue) and 7-day posttreatment (red) conditions shown in Figs. 2A-D, indicated that OHC injury preferably occurred for the high-frequency region, and the injury expanded to lower frequency regions as the overall ototoxic severity escalated. Similar to the aforementioned inter-animal variability observed in ABR thresholds, OHC injury was also highly variable according to DPOAE measures. For example, for one mouse treated with the same 200G/200F dose, severe OHC damage as indicated in Fig. 2F was observed, while the other mouse might exhibit normal DPOAE responses at 7 days posttreatment. Based on the severity of OHC injuries, we categorized G/F-induced cochleotoxicity into three types. In the mild type, OHC damage represented, for example, in Fig 2B, was limited to the extreme high-frequency range (>30 kHz). In the moderate type shown in Fig. 2C, OHC damage spread into the mid-frequency range (~20 kHz or lower). In the severe type indicated in Fig. 2D, OHC damage was seen throughout the cochlea. Among five mice exhibiting severe DPOAE deficits, four of them involved bilateral injuries as shown for mouse #248 in Fig. 2D, and mouse #387 in Fig. 2F. This observation was in accordance with the consensus that aminoglycoside-induced ototoxicity typically affects both ears equally (Forge and Schacht, 2000). Yet, unilateral mild high-frequency OHC injury was not rare in the present study, as the contralateral showing no sign of DPOAE deficit. Here, the upper-frequency limitation of f_2 stimuli was 64 kHz, whereas DPOAE levels were frequently indistinguishable from the NF as observed for the data present in Fig. 2. This technical upper-frequency boundary was very close to, but not adequately reaching the extremity of the basal cochlear location. As a result, OHC injury at the extreme basal cochlear region could not be detected, and an ear could be mis-identified as normal by DPOAE measurements.

The results from ABR thresholds and DPOAE measures, *in toto*, indicated that we have generated a broad spectrum of cochlear injuries based on various G/F dosing combinations, which allowed us to interrogate the ribbon synapse for possible synaptic damage that is independent of HC injuries.

3.2 The wave I I/O curve of ABR responses

ABR wave I amplitude is deemed as a legitimate non-invasive physiological indicator of the functionality of the afferent AN, including the ribbon synapses. As ABR thresholds in G/F-treated mice were measured, the wave I I/O function was also routinely acquired at 12 kHz with a broad range of sound levels as illustrated in Fig. 3. For lower G/F dosages, including the 200G/50F one shown in Fig. 3A, the 200G/100F dose of Fig. 3B and the 200G/200F one in Fig. 3C, no severe OHC injury was observed based on DPOAEs, and the complete range of wave I amplitudes could be acquired as well. The group average of posttreatment wave I I/O functions, at 3 and 7 days, were never lower than their pretreatment control-function counterparts. These data suggested the ribbon synapses, at the tested frequency location, were resistant to G/F treatments. For the 200G/400F dose, for group averaging purposes, wave I amplitudes were assigned by zeros for sub-threshold ABR waveforms. Only with the contribution of "zero assignments", the average posttreatment wave I I/O curves were lower than the pretreatment curves.

Thus, if the hearing sensitivity at the testing frequency of 12 kHz remained after G/F treatment, ABR wave I amplitude was not reduced. Yet, focusing only at the higher-sound levels, wave I amplitudes actually increased for certain treatment conditions and were more significant at earlier posttreatment time points, for instance, at the 200G/50F dose shown in Fig. 3A (2-way ANOVA, 3-day *vs.* pre, $F(1,40)=11.42$, $p=0.0016$; 7-day *vs.* pre, $F(1,40)=4.126$, $p=0.049$). To further investigate the underlying mechanism of the wave I amplitude increment, wave I I/O functions were regrouped by the severity of OHC injuries, *i.e.* DPOAE deficit, as shown in Figs. 3E-G. Intriguingly, it was the ears with moderate OHC injury, instead of the ears with mild injury, exhibiting increased wave I amplitudes at higher sound levels as demonstrated in Fig. 3G, for example (2-way ANOVA, 3-day *vs.* pre, $F(1,129)=8.985$, $p=0.0033$; 7-day *vs.* pre, $F(1,129)=3.550$, $p=0.0618$).

Results from DPOAE measurements and ABR responses, including both ABR thresholds and wave I amplitudes, collectively, indicated that 400 mg/kg furosemide dosing represents an unfavorable dosage to pursue synaptic damage independent of HC loss.

3.3 Morphological alteration of synaptic ribbon after G/F treatment

Seven days after the one-time G/F treatment, synaptic ribbons that were identified by the anti-CtBP2 labeling exhibited various degrees of morphological change. On the *xy* plane at the cochlear location equivalent to 12 kHz (Muller et al., 2005), the ribbon distribution appeared normal for some low-dose G/F treatments, demonstrated by a vacant zone basally located to the IHC nuclei, without a

reduction in the number of ribbons, *i.e.*, ribbon density, as illustrated by the micrographs of Figs. 4A1-A4. Among them, Figs. 4A2-A4 are the confocal images reconstructed in the *yz* plane from three adjacent IHCs. Similar to our previous findings in healthy control cochleae, the size of ribbons near the nuclei was relatively small, while those located at the IHC basal pole were larger (Edderkaoui et al., 2018). In addition, it is noteworthy that with the mounting technique used, the IHCs from the apex and the middle coils of the cochlea generally orientate in parallel to the cover slide, which allowed a convenient quantifying of the distance of individual ribbons to the nucleus along the *y* axis, *i.e.*, the main axis of the IHC. Thus, a shape of normal distribution along the main axis was typically anticipated, as indicated in Fig. 4A5. Yet, under most G/F treatment conditions, a certain distribution disorder was observed, for example, in Figs. 4B1-B5, manifested by some ribbons being shifted toward the IHC nucleus without a reduction in the number of ribbons. In addition, the "nucleus-ward or upward" shift appeared predominantly toward the pillar side of the IHC as shown on the left side of Figs. 4B2 and 4B4. The axial gradient based on the ribbon size was also disturbed. In the extreme ototoxic scenario, the ribbon numbers did decline after some high-dose G/F treatments, with extensive upward shift of the ribbons as illustrated in Fig. 4C2, and enlarged ribbons in many cases as demonstrated in Fig. 4C1. More examples showing the axial distribution of synaptic ribbons, ranging from normal to extensive upward shift, with and without reduction in ribbon density can be seen in Suppl. Fig. 3.

3.4 OHC damage occurs in between synaptic plasticity and ribbon density reduction

The ribbon numbers per IHC, *i.e.*, ribbon density, was quantified systemically at the 12-kHz cochlear location and number reduction was rare, only occurring in some cases with the highest G/F dosings at 200G/400F (see Fig. 5A) and 400G/200F (see Fig. 5B), although the reduction was not significant in either dosing group due to inter-animal variations. Otherwise, G/F treatment typically resulted in a marginal increase in ribbon density, a hallmark of synaptic plasticity, and the increment was statistically significant for the 200G/200F group (Figs. 5A and B; p=0.006, unpaired t-test with Welch's correction). Thus, combining with the ABR and DPOAE results, the data collectively suggest that the reduction of ribbon density only occurred in the situation with substantial cochlear damage due to G/F treatment, summarized by Fig. 5C. When the ribbon dataset was sorted according to the severity of OHC damage (*i.e.*, DPOAE damage) that was defined earlier, the reduction became significant with severe DPOAE deficit as shown in Fig. 5D (p=0.004, unpaired t-test with Welch's correction).

Cochlear tissue was typically processed with anti-Myo7a antibodies and/or phalloidin in addition to anti-CtBP2 antibodies, in order to address HC integrity at the same cochlear location where the synaptic ribbons were assessed. With our treatment protocols and doses, G/F-induced IHC loss was extremely rare, while OHC loss frequently was extreme at each imaged cochlear location. That is, the OHC loss was often either complete or none, as shown in Fig. 6A. Thus, the cochlear samples at each examined location could be characterized into one of the two groups, "no OHC loss" group *vs.* "OHC loss" group. As partially reported earlier, 7 days after 200G/200F treatment, the overall ribbon density was elevated at examined locations, a sign of synaptic plasticity, including at 12-, 32- and 48-kHz locations as shown in Fig. 6B (2-way ANOVA, $F(1,21)=9.15$, $p=0.0064$). Intriguingly, the G/F-induced increment in ribbon density was exclusively contributed by the samples exhibiting "no OHC loss" as illustrated in Fig. 6C (2-way ANOVA, $F(1,17)=44.75$, $p<0.0001$). Representative cochlear samples at the 12-kHz location from "no OHC loss" group (see Fig. 6E) and "OHC loss" group (see Fig. 6F) showed OHC conditions in accordance with the DPOAE results on the same ear measured immediately prior to tissue collection, shown in Figs. 2E and 2F, respectively. Corresponding values of the ribbon density are depicted in Fig. 6D. Note that without identifiable OHC survival, the ribbon density still fell into the normal range for non-G/F-treated control samples, further confirming that OHC structural damage occurred prior to a ribbon-density reduction.

3.5 Gentamicin/furosemide-induced ribbons unlikely functional

The marginal increase in ribbon density indicated a small number of synaptic ribbons were newly formed after the titrated G/F treatment. The physiological significance of this morphological alteration is unclear. According to the observation that the G/F-induced elevation of the ABR wave I I/O function was slightly more overt by 3 days posttreatment compared to 7 days as indicated in Fig. 3, we speculated that the G/F-enhanced ribbon density also occurred at earlier time points following treatment. Thus, we focused on a subset of *C57BL/6* mice that were administered with 400G/200F doses, and had their cochlear tissue harvested 2 days posttreatment, to better understand the mechanism of the newly generated, G/F-induced synaptic ribbons. The selected group of mice exhibited normal ABR thresholds 2 days after treatment (data not shown), but elevated wave-I amplitudes across the entire range of the tested sound levels as illustrated in Fig. 7A (2-way ANOVA, $F(1, 151)=6.827$, $p=0.0099$). In addition, the ribbon density appeared increased at multiple locations throughout the cochlea as indicated in Fig. 7B. However, when we interrogated the correlation

between the ABR wave-I amplitude and the ribbon density from individual cochleae at the 12-kHz location, the correlation coefficient was low (see Fig. 7C, R^2=0.14). This outcome was further confirmed from the larger, 7-day post treatment dataset shown in Fig. 7D. Here, except for the extremely low ribbon numbers (*i.e.*, two incidences) that corresponded to the unidentifiable wave I, the G/F-enhanced ribbon density did not result in increased wave-I amplitudes with a coefficient index near 0. Consequently, the lack of correlation between the electrophysiologic measures and the morphological quantification indicated that the newly G/F-induced ribbons did not directly contribute to the elevated wave-I amplitude, and the synaptic plasticity based on morphological observations was not functional in the present study.

4. Discussion

Similar to acoustic overstimulation and aging, it has long been considered that the primary ototoxic target of aminoglycosides including gentamicin is the sensory hair cells in the mammalian cochlea, while the damage to the SGNs is secondary (Forge and Schacht, 2000; Hirose and Sato, 2011). This dogma has recently been challenged (Liberman and Kujawa, 2017; Ruan et al., 2014), particularly with the recent research interest in HHL, a unique form of auditory neuropathy (Starr and Rance, 2015), in which the temporal processing capacity is drastically compromised, while sensitivity to pure tones remains intact.

In the present study, we used DPOAE methods to measure OHC integrity along with morphological counter-labeling agents including phalloidin and anti-Myo7a to identify sensory HCs. DPOAE measures are fast and reliable and, more importantly, a non-invasive approach to evaluate OHC function, and allowing multiple assessment time points upon G/F treatment. Thus, we could readily observe the progress of G/F-induced cochleotoxicity. Together with immunofluorescence techniques, the present study concluded that the G/F treatment did alter the distribution of synaptic ribbons in the IHC, but more likely in a neuroplasticity fashion instead of in an HHL manner, prior to damage to the OHCs.

4.1 Gentamicin/furosemide treatment as an effective ototoxicity model in mice

A single dose of gentamicin combined with 400 mg/kg of furosemide is widely used as an effective experimental strategy to ablate OHCs in the inner ear (Kraft et al., 2013; Ruan et al., 2014; Schmitz et

al., 2014). In the present study, DPOAE responses confirmed that G/F treatment resulted in HC damage, with equivalent damage severity bilaterally (Forge and Schacht, 2000). Based on our observations, unilateral severe ototoxic damage is extremely rare with only one observed case. This drug-induced cochlear damage has been used as a disease model to study corrective approaches such as cochlear implantation and HC regeneration (Kraft et al., 2013). Since we were keen on producing damage specific to the synaptic ribbon without HC loss, a variety of titrated dose combinations between gentamicin and furosemide were used (see Suppl. Fig. 1). The overall results indicated that the 400 mg/kg dosage was on the high side of dose selection that frequently caused OHC damage. Between the conditions of 200G/400F and 400G/200F, the latter was gentler in terms of stressing OHCs.

From both experimental animal studies and human temporal bone histology, furosemide and other loop diuretics exert reversible damage or edema to the cochlear lateral wall and the stria vascularis within it (Ding et al., 2016; Rybak, 1993; Santos and Nadol, 2017). The edema is typically manifested by the enlargement of the extracellular spaces from the marginal cell tight junctions to the basal cell layer with broadening the stria vascularis. Diuretics alone do not directly damage HCs in the cochlea and the vestibular system, but, rather, cause a secondary effect from changes in the stria vascularis. Studies in mice suggested that furosemide targets the renin-angiotensin aldosterone system in the stria vascularis and disrupts the blood-cochlear barrier (Ding et al., 2016; Rybak, 1993), which allows ototoxins such as gentamicin to flush into the endolymphatic space many times more than the regular volume, and to quickly enter HCs from there (Li and Steyger, 2011). The effectiveness of furosemide on the stria vascularis likely forms a gradient from the cochlear apex to the base (Hirose and Sato, 2011), while the cochleotoxicity of gentamicin forms a gradient from base to apex. The combined ototoxic efficacy of G/F treatment appears more towards the cochlear base, similar to findings previously reported with kanamycin/furosemide treatment (Hirose and Sato, 2011). Yet, an exception did occur and a few individual cases showed apical-only G/F ototoxicity (DPOAE data not shown). In addition, G/F-induced IHC loss was rare in the present study, given the examination time points were no more than 2 weeks after treatment. Thus, this treatment protocol produces a good model for research efforts on cochlear electrode implantation and regeneration of OHCs.

4.2 Using wave-I amplitude to estimate ribbon density was not practical after gentamicin/furosemide treatment

Firstly, as shown in Fig. 3, we did observe a marginal G/F-enhanced wave-I amplitude from group data, and the increment appeared more evident from the ears exhibiting moderate DPOAE deficit as illustrated in Fig. 3G. It is established that a correlation exists between the wave-I ABR amplitude and ribbon density in age-related and/or noise-induced HHL (D et al., 2020). However, when we pooled data from ears with both ABR wave-I measurement and ribbon quantification at the 12-kHz location, this correlation did not exist for individual G/F-treated ears as seen in Figs. 7C and D as new synaptic ribbons formed. In addition, based on our observations, the prevalence of G/F-enhanced ribbon density was greater than that of G/F-increased wave-I amplitudes. One reason, of course, could be due to the lack of stability of ABR measurements. Or alternatively, the newly formed ribbons were not functional in our protocol and the increased wave-I amplitudes were supported by the augmentation of other functional modalities within the cochlea. For instance, the loss of sensory input from damaged HCs at higher-frequency locations can modify the tuning of succeeding SGNs, resulting in an increased population of SGNs responding to sounds at adjacent lower frequencies, and, consequently, a greater wave-I amplitude. This acute auditory effect is termed the "edge effect" (Snyder et al., 2000). The fact that ears with moderate DPOAE deficit exhibit greater G/F-enhanced wave-I amplitudes at the 12-kHz location supports this explanation, given that the 12-kHz location in these cases were closer to the OHC injury "edge" as indicated in Figs. 3G and 2C. This acute effect could fade away to a certain extent as the succeeding SGNs gradually lost their function due to the loss of intended input from the corresponding sensory epithelium. Concordantly, the fact that 7-day wave-I amplitude elevations were slightly less than that of the 3-day elevations did support the hypothesis as corroborated in Fig. 3.

4.3 Pillar-side upward shift of synaptic ribbons with G/F treatment

After G/F treatment in *C57BL/6* mice, pillar-side upward shift of synaptic ribbon is a prevalent morphological event, as illustrated in Fig. 8. The marginally increased number of ribbons appear not adequate to be solely responsible for their upward shift. That is, the shifted ribbons are unlikely the newly generated synaptic ribbons, but, rather, are the relocated ribbons from the basal pole of IHCs. Specimens processed with both CtPB2 and GluR2 antibodies confirmed the expected pairing between the presynaptic ribbon and postsynaptic AMPA receptor (Figs. 4A4 and 4B4, and Suppl. Fig. 4), which suggests that the ribbons are mature, instead of freshly assembled. However, if the overall ribbon density increased significantly with G/F treatment, it is reasonable to hypothesize that some new ribbons are recruited to the cellular membrane not far from the nucleus. Ribbons that are located on the

pillar side are considered to connect with ANFs with low-threshold and high-spontaneous discharge rates. These fibers also present a narrow dynamic range of discharge rate, meaning less of an increment in the overall discharge rate as the sound level of the acoustic stimulus increased. This could partially explain the marginal, and mostly non-significant increase of the ABR wave-I amplitudes shown in Fig. 3, as well as the lack of a correlation between the wave I amplitudes and ribbon density.

4.4 Why was not there HHL-type of reduction of ribbon density?

Ribbon synaptic transmission between IHCs and SGNs is excitatory and glutamatergic, and the ribbon synapse is susceptible to excitotoxicity, presumably due to excessive glutamate release from IHCs. Intracochlear perfusion of glutamate agonists *in vivo* results in the degeneration of SGN synaptic terminals on IHCs (Pujol et al., 1996; Pujol et al., 1985; Ruel et al., 2007). To date, excitotoxicity is the leading underlying mechanism of the HHL-type synaptopathy due to acoustic overexposure (Kujawa and Liberman, 2009, 2015). Intriguingly, excitotoxicity has also been proposed as one of the toxic mechanisms impeding auditory function with aminoglycoside treatment (Duan et al., 2000; Sedo-Cabezon et al., 2014). Given that excitotoxicity primarily targets the synaptic terminals of ANFs, *i.e.*, ribbon synapses, it is legitimate to speculate that aminoglycosides could cause synaptopathy, and more specifically, an HHL-type of synaptopathy with carefully titrated doses of aminoglycosides (Jiang et al., 2017; Liberman and Kujawa, 2017). In the present study, with combined G/F treatment, synaptic ribbons were often reorganized, and ribbon density was rarely reduced, at least, not prior to overt damage at the OHC level. This observation is contrary to a model of aminoglycoside-induced excitotoxicity. Since the cochlear damage by a furosemide-induced ototoxicity is rather rapid (Taylor et al., 2008), we postulate that a chronic situation is necessary for the aminoglycoside to be effectively excitotoxic at the synaptic terminals of the ANF, thus, multiday aminoglycoside treatment might be necessary to encourage an adequate excitotoxicity that results in an HHL-type synaptopathy. Further investigations are thus warranted to confirm such a notion.

Conflict of Interest Statement

The authors declare that the research was conducted in the absence of any commercial or financial relationships that could be construed as a potential conflict of interest.

Acknowledgement

This material is the result of work was partly supported by the Office of the Assistant Secretary of Defense for Health Affairs through the Peer Reviewed Medical Research Program under Awards No. W81XWH-14-1-0006 (HL) and No. W81XWH-19-1-0862 (ML), and by the Office of Research & Development of Veterans Health Association under Award No. RX002813 (HL). This work is also supported with resources and the use of facilities at the VA Loma Linda Healthcare System. Opinions, interpretations, conclusions and recommendations are those of the authors and are not necessarily endorsed by the U.S. Department of Defense, the Department of Veterans Affairs or the United States Government. In addition, the authors like to express their sincere gratitude to Brenda Lonsbury-Martin for constructive comments on the manuscript.

Reference

Basile, A.S., Huang, J.M., Xie, C., Webster, D., Berlin, C., and Skolnick, P. (1996). N-methyl-D-aspartate antagonists limit aminoglycoside antibiotic-induced hearing loss. Nat Med *2*, 1338-1343.

D, C.K., Wan, G., Cassinotti, L., and Corfas, G. (2020). Hidden Hearing Loss: A Disorder with Multiple Etiologies and Mechanisms. Cold Spring Harb Perspect Med *10*.

Ding, D., Liu, H., Qi, W., Jiang, H., Li, Y., Wu, X., Sun, H., Gross, K., and Salvi, R. (2016). Ototoxic effects and mechanisms of loop diuretics. J Otol *11*, 145-156.

Duan, M., Agerman, K., Ernfors, P., and Canlon, B. (2000). Complementary roles of neurotrophin 3 and a N-methyl-D-aspartate antagonist in the protection of noise and aminoglycoside-induced ototoxicity. Proc Natl Acad Sci U S A *97*, 7597-7602.

Edderkaoui, B., Sargsyan, L., Hetrick, A., and Li, H. (2018). Deficiency of Duffy Antigen Receptor for Chemokines Ameliorated Cochlear Damage From Noise Exposure. Frontiers in Molecular Neuroscience *11*.

Forge, A., and Schacht, J. (2000). Aminoglycoside antibiotics. Audiol Neurootol *5*, 3-22.

Hirose, K., and Sato, E. (2011). Comparative analysis of combination kanamycin-furosemide versus kanamycin alone in the mouse cochlea. Hear Res *272*, 108-116.

Hong, J., Chen, Y., Zhang, Y., Li, J., Ren, L., Yang, L., Shi, L., Li, A., Zhang, T., Li, H.*, et al.* (2018). N-Methyl-D-Aspartate Receptors Involvement in the Gentamicin-Induced Hearing Loss and Pathological Changes of Ribbon Synapse in the Mouse Cochlear Inner Hair Cells. Neural Plast *2018*, 3989201.

Izumikawa, M., Minoda, R., Kawamoto, K., Abrashkin, K.A., Swiderski, D.L., Dolan, D.F., Brough, D.E., and Raphael, Y. (2005). Auditory hair cell replacement and hearing improvement by Atoh1 gene therapy in deaf mammals. Nat Med *11*, 271-276.

Jiang, M., Karasawa, T., and Steyger, P.S. (2017). Aminoglycoside-Induced Cochleotoxicity: A Review. Front Cell Neurosci *11*, 308.

Kraft, S., Hsu, C., Brough, D.E., and Staecker, H. (2013). Atoh1 induces auditory hair cell recovery in mice after ototoxic injury. Laryngoscope *123*, 992-999.

Kujawa, S.G., and Liberman, M.C. (2009). Adding insult to injury: cochlear nerve degeneration after "temporary" noise-induced hearing loss. J Neurosci *29*, 14077-14085.

Kujawa, S.G., and Liberman, M.C. (2015). Synaptopathy in the noise-exposed and aging cochlea: Primary neural degeneration in acquired sensorineural hearing loss. Hear Res *330*, 191-199.
Li, H., and Steyger, P.S. (2011). Systemic aminoglycosides are trafficked via endolymph into cochlear hair cells. Sci Rep *1*.
Liberman, M.C., and Kujawa, S.G. (2017). Cochlear synaptopathy in acquired sensorineural hearing loss: Manifestations and mechanisms. Hear Res *349*, 138-147.
Liu, K., Chen, D., Guo, W., Yu, N., Wang, X., Ji, F., Hou, Z., Yang, W.Y., and Yang, S. (2015). Spontaneous and Partial Repair of Ribbon Synapse in Cochlear Inner Hair Cells After Ototoxic Withdrawal. Mol Neurobiol *52*, 1680-1689.
Liu, K., Jiang, X., Shi, C., Shi, L., Yang, B., Shi, L., Xu, Y., Yang, W., and Yang, S. (2013). Cochlear inner hair cell ribbon synapse is the primary target of ototoxic aminoglycoside stimuli. Mol Neurobiol *48*, 647-654.
Moser, T., and Starr, A. (2016). Auditory neuropathy--neural and synaptic mechanisms. Nat Rev Neurol *12*, 135-149.
Muller, M., von Hunerbein, K., Hoidis, S., and Smolders, J.W. (2005). A physiological place-frequency map of the cochlea in the CBA/J mouse. Hear Res *202*, 63-73.
Oishi, N., Duscha, S., Boukari, H., Meyer, M., Xie, J., Wei, G., Schrepfer, T., Roschitzki, B., Boettger, E.C., and Schacht, J. (2015). XBP1 mitigates aminoglycoside-induced endoplasmic reticulum stress and neuronal cell death. Cell Death Dis *6*, e1763.
Pujol, R., Gervais d'Aldin, C., Saffiedine, S., Eybalin, M., and Puel, J.L. (1996). Repair of inner hair cell-auditory nerve synapses and recovery of function after an excitotoxic injury. In Auditory plasticity and regeneration, RJS, ed. (New York: Thieme Medical Publishers Inc), pp. 100-107.
Pujol, R., Lenoir, M., Robertson, D., Eybalin, M., and Johnstone, B.M. (1985). Kainic acid selectively alters auditory dendrites connected with cochlear inner hair cells. Hear Res *18*, 145-151.
Ruan, Q., Ao, H., He, J., Chen, Z., Yu, Z., Zhang, R., Wang, J., and Yin, S. (2014). Topographic and quantitative evaluation of gentamicin-induced damage to peripheral innervation of mouse cochleae. Neurotoxicology *40*, 86-96.
Ruel, J., Wang, J., Rebillard, G., Eybalin, M., Lloyd, R., Pujol, R., and Puel, J.L. (2007). Physiology, pharmacology and plasticity at the inner hair cell synaptic complex. Hear Res *227*, 19-27.
Rybak, L.P. (1993). Ototoxicity of loop diuretics. Otolaryngol Clin North Am *26*, 829-844.
Santos, F., and Nadol, J.B. (2017). Temporal bone histopathology of furosemide ototoxicity. Laryngoscope Investig Otolaryngol *2*, 204-207.
Schmitz, H.M., Johnson, S.B., and Santi, P.A. (2014). Kanamycin-furosemide ototoxicity in the mouse cochlea: a 3-dimensional analysis. Otolaryngol Head Neck Surg *150*, 666-672.
Sedo-Cabezon, L., Boadas-Vaello, P., Soler-Martin, C., and Llorens, J. (2014). Vestibular damage in chronic ototoxicity: a mini-review. Neurotoxicology *43*, 21-27.
Segal, J.A., Harris, B.D., Kustova, Y., Basile, A., and Skolnick, P. (1999). Aminoglycoside neurotoxicity involves NMDA receptor activation. Brain Res *815*, 270-277.
Snyder, R.L., Sinex, D.G., McGee, J.D., and Walsh, E.W. (2000). Acute spiral ganglion lesions change the tuning and tonotopic organization of cat inferior colliculus neurons. Hear Res *147*, 200-220.
Spongr, V.P., Flood, D.G., Frisina, R.D., and Salvi, R.J. (1997). Quantitative measures of hair cell loss in CBA and C57BL/6 mice throughout their life spans. J Acoust Soc Am *101*, 3546-3553.
Starr, A., and Rance, G. (2015). Auditory neuropathy. Handbook of clinical neurology *129*, 495-508.
Taylor, R.R., Nevill, G., and Forge, A. (2008). Rapid hair cell loss: a mouse model for cochlear lesions. J Assoc Res Otolaryngol *9*, 44-64.
Willott, J.F., Turner, J.G., Carlson, S., Ding, D., Seegers Bross, L., and Falls, W.A. (1998). The BALB/c mouse as an animal model for progressive sensorineural hearing loss. Hear Res *115*, 162-174.

Figure legends

Figure 1: Dose response of G/F treatment as determined by ABR thresholds. A: Average ABR thresholds with 200G/0F treatment measured before, 3-day and 7-day posttreatment. **B**: 200G/50F. **C**: 200G/100F. **D**: 200G/400F. N=2-5 mice per group, both ears tested. Error bar=SEM. **E**: Selected ABR thresholds from individual ears measured at 3-day posttreatment, and **F**: at 7-day posttreatment.

Figure 2: DPOAE revealed OHC damage from G/F treatment in individual mice. In the fixed dose of gentamicin groups, the introduction of furosemide at varied doses caused a DPOAE deficit in the cochlea at various degrees of severity, from **A**: no damage, to **B**: mild damage, **C**: moderate damage, and **D**: severe damage 7-day posttreatment. Considerable inter-animal variation existed with the same treatment regimen. For instance, both with 200G/200F treatment, **E**: no DPOAE deficit were observed in mouse #388 7-day posttreatment, while **F**: severe functional damage was observed in mouse #387. Sound levels of the primary tones were equal at L_1=L_2=55 dB SPL, f_2/f_1=1.25. NF=noise floor.

Figure 3: Input/output functions (I/Os) of wave-I amplitude from ABR to 12-kHz tones. A: Average ABR wave I amplitude I/O functions with 200G/50F treatment measured before, 3-day and 7-day posttreatment. **B**: 200G/100F. **C**: 200G/200F. **D**: 200G/400F. **E**: Average I/O functions from cochleae with no DPOAE deficit, **F**: mild DPOAE decrements, and **G**: moderate DPOAE losses. N=2-4 mice per group, both ears tested. Error bar=SEM.

Figure 4: Alteration of synaptic ribbons after G/F treatment. A: In the apical and middle cochlear locations free of OHC damage, low-dose G/F treatment might not induce any visible change in CtBP2-labeled synaptic ribbons (red puncta), showing a characteristic vacant zone depicted by brackets and dotted lines basal to the IHC nucleus in the *xy* plane (**A1**). Error bar=20 μm. Reconstructed images in the *yz* plane from three adjacent IHCs exhibited the distribution of ribbons along the pillar-modiolar axis (**A2**), with identification of the cytoplasm of the IHC by anti-Myo7a immunolabeling (**A3**, blue), and paired postsynaptic AMPA receptors by anti-GluR2 immunolabeling (**A4**, green). A semi-normal distribution of the ribbon along the main cell axis was often observed (**A5**). **B1-4**: Seven days after G/F treatment, at cochlear locations free of OHC damage, a pillar-side upward shift of synaptic ribbons was often seen without a reduction in ribbon number. **B5**: ribbon distribution along the main cell axis was skewed to the nucleus. **C1**: With severe cochlear damage induced by G/F treatment, the ribbon density could be drastically reduced and many individual ribbons enlarged (arrowhead), and again, often exhibiting an upward shift (**C2**).

Figure 5: Group analysis of synaptic ribbon density after G/F treatment. A: Ribbon density with a fixed dose of gentamicin and varied dose of furosemide. N is identified in each column. **B**: Ribbon density with fixed doses of furosemide and varied doses of gentamicin. **C**: Illustration of G/F treatment dosages that modified ribbon density. **D**: Ribbon density is categorized based on the severity of DPOAE deficit. ** $p< 0.01$, 2-tailed Welch's t test. Error bar=SD.

Figure 6: Synaptic ribbon density after 200G/200F treatment. A: The OHC loss at each cochlear location where a confocal image acquired, was often complete or none. **B**: Average ribbon density from multiple cochlear locations 7 days posttreatment. Error bar=SD. **C**: Ribbon density grouped by whether OHCs were largely survived at the same cochlear location. **D**: Ribbon densities from

individual cochleae at the 12-kHz location. Red: showing OHC loss. Green: without OHC loss. **E**: A representative confocal image showing intact OHCs and an elevated number of synaptic ribbons. Scale bar=10 μm. **F**: A representative confocal image showing a complete loss of OHCs. Phalloidin labeling (green) identified scar formation at the sites of missing OHCs.

Figure 7: The lack of correlation between the wave-I ABR amplitudes and ribbon density. A: Average ABR I/O-amplitude functions for 400G/200F treatment measured before (N=8) and 2 days posttreatment (N=6). Error bar=SEM. **B**: Average ribbon density from multiple cochlear locations 2-day posttreatment (N=5-11). Error bar=SD. **C**: Scatter plot indicates the lack of correlation between wave-I ABR amplitude and ribbon density from individual cochleae for the 400G/200F treatment at 2 days posttreatment. Gray zone indicates the ribbon density from control ears, ±1 SD. **D**: Scatter plot shows poor correlation coefficient between the wave I ABR amplitude and the ribbon density, from individual cochleae with intact OHCs, treated by 200 mg/kg gentamicin and varied furosemide at 7-day posttreatment.

Figure 8: Illustration demonstrates the pillar-side upward shift of the synaptic ribbons after G/F treatment. Red particles depict individual synaptic ribbons. p=pillar side; m=modiolar side.

Supplementary Materials

Supplemental Figure 1: G/F dose combinations applied to *C57BL/6* in the present study.

Supplemental Figure 2: Average ABR thresholds to the G/F treatment of 0G/200F (**A**), 50G/200F (**B**), 100G/200F (**C**), and 200G/200F (**D**).

Supplemental Figure 3: Ribbon distribution along the main IHC axis in the normal formation (**A**), or presenting an upward shift without a reduction of ribbon density (**B**), or with a drastic reduction (**C**).

Supplemental Figure 4: Postsynaptic AMPA receptors were identified by anti-GluR2 immunolabeling. The pre- and post-synaptic pairing were typically maintained after G/F treatment when OHCs were survived at the same examined region, either with (**B**) or without upward shift of the synaptic ribbons (**A**). However, unpairing did occur after the OHC loss (**C**), detected by phalloidin labeling (blue). Error bar=20 μm.